Towards efficient and generic entanglement detection

Jue Xu[*] and Qi Zhao[†]
(Dated: September 18, 2022)

Detection of entanglement structure is an indispensable step for practical quantum computation and communication. In this work, we compare complexity and performance of several recently-developed methods, including entanglement witness methods, shadow tomography, classical machine learning, and quantum algorithms (circuits). We illustrate the advantages and limitations of machine learning and quantum algorithms.

CONTENTS

I. INTRODUCTION

Entanglement [1] is the key ingredient of quantum computation [], quantum communication [], and quantum cryptography []. For practical purpose, it is essential to benckmark (characterize) multipartite entanglement structures of target states. We review the recently developed methods to entanglement detection: entanglement witness [2], shadow tomography [3], classical machine learning [4], and quantum (variational/circuit) algorithms [5].

However, decoherence is inevitable in real-world, which means the interaction between a quantum system and classical environment would greatly affect entanglement quality and diminish quantum advantage. So, detecting or benchmarking entanglement is essential in actual experiments. Our goal is to find an efficient and generic way to do it. Roughly speaking, our solution is to make use of both machine learning techniques and some recently-developed

---

[*] juexu@cs.umd.edu
[†] zhaoqi@cs.hku.hk

quantum algorithms. Explicitly, our pipeline starts with a tomographic entanglement witness ansatz which is the linear combination of all possible n-qubit pauli operators. Next, we generate random density matrices with labels for training. Then, we need to estimate the expectation values of each pauli operator, which are features for training a classical SVM. Probably, we can eliminate unimportant features, which means we might not need all pauli operators in our generic witness. Finally, we test and make predictions with brand new samples. We would test our pipeline in actual experiments.

II. PRELIMINARIES

Notation 1. The hats on the matrices such as $\hat{H}$, O, W, emphasize that they play the roles of operators (Hermitian matrices). density matrix ρ (omitted) $\{I, X, Y, Z\}$

Notation 2. In the machine learning setting, denote vector (matrix) $\mathbf{x}$, $\mathbf{w}$, $\mathbf{K}$ by boldface font.

Notation 3. If no ambiguity, we omitted the tensor product for readability, that is, $|\psi_A\rangle |\psi_B\rangle \equiv |\psi_A\rangle \otimes |\psi_B\rangle$ and $\hat{X}^{(1)}\hat{Z}^{(3)} \equiv \hat{X} \otimes \mathbb{1} \otimes \hat{Z}$.

A. Entanglement structures

Large scale entanglement is the (main) resource of quantum advantages in quantum computation and communication. Firstly, we consider the simplest entanglement structure: bipartite separable case.

Definition 1 (bipartite separable). Consider a bipartite system AB with the Hilbert space $\mathcal{H}_A \otimes \mathcal{H}_B$, where $\mathcal{H}_A$ has dimension d_A and $\mathcal{H}_B$ has dimensional d_B, respectively. A pure state is bipartite (bi-)separable if it is in a tensor product form $|\psi\rangle_{bi} = |\phi\rangle_A \otimes |\phi\rangle_B$, where $\mathcal{P}_2 = \{A, B\}$ is a bipartition of the qubits in the system. A mixed state ρ is separable iff it can be written as a convex combination of pure biseparable states with probability distribution $\{p_i\}$

$$\rho_{bi} = \sum_i p_i |\psi_i\rangle\langle\psi_i|_{bi}, \ \forall p_i > 0, \sum_i p_i = 1 \tag{1}$$

where $|\psi_i\rangle$ may be biseparable with respect to different partitions (otherwise genuine multipartite entanglement). Otherwise, ρ_{AB} is entangled.

Note that the state $|\phi\rangle_A$ may be entangled, thus the state $|\psi\rangle$ is not necessarily fully separable. The simple statement "The state is entangled" would still allow that only two of the qubits are entangled while the rest is in a product state. Note that each separable state $|\psi\rangle_{bi}$ in the summation can have different bipartitions. The separable state set is denoted as S_b. There is another restricted way for the extension to mixed states. A state is $\mathcal{P}_2$-separable, if it is a mixing of pure separable states with a same partition $\mathcal{P}_2$, and we denote the state set as $S_b^{\mathcal{P}_2}$. Many methods [6] have been developed to determine whether a state is bi-separable.

Theorem 1 (PPT criterion [7]). *The positive partial transpose (*PPT*) criterion saying the state is entangled iff the smallest eigenvalue of partial transpose $\rho_{AB}^{\mathsf{T}_A}$ is negative. So, a separable state (bipartite separable) must have PPT (the partially transposed (PT) density matrix $\rho_{AB}^{\mathsf{T}_A}$ is positive, semidefinite). Note, it is only necessary and sufficient when $d_A d_B \leq 6$. PPT is necessary condition for bi-separable.*

For multipartite quantum systems, it is crucial to identify not only the presence of entanglement but also its detailed structure. An identification of the entanglement structure may thus provide us with a hint about where imperfections in the setup may occur, as well as where we can identify groups of subsystems that can still exhibit strong quantum-information processing capabilities.

Given a n-qubit quantum system and its partition into m subsystems, the *entanglement structure* indicates how the subsystems are entangled with each other. In some specific systems, such as distributed quantum computing[] quantum networks[] or atoms in a lattice, the geometric configuration can naturally determine the system partition. Therefore, it is practically interesting to study entanglement structure under partitions.

Definition 2 (fully separable). An n-qubit pure state $|\psi_f\rangle$ is *fully separable* iff(, and is (fully) n-separable if it is in S_n). An n-qubit pure state $|\psi_f\rangle$ is $\mathcal{P}$-fully separable iff it can be written as $|\psi_f\rangle = \otimes_i^m |\phi_{A_i}\rangle$. Analoguous to Eq. (1), an n-qubit mixed state ρ_f is $\mathcal{P}$-fully separable iff it can be decomposed into a convex mixture of $\mathcal{P}$-fully separable pure states. P-bi-separable... $S_f^{\mathcal{P}} \subset S_b^{\mathcal{P}}$

define fully- and biseparable states with respect to a *specific partition* $\mathcal{P}_m$

Definition 3 (fully entangled)**.** An n-qubit quantum state ρ is a *fully entangled*, if it is outside of the separable state set $S_b^{\mathcal{P}_2}$ for any partition, $\rho \notin S_b^{\mathcal{P}_2}, \forall \mathcal{P}_2 = \{A, \bar{A}\}$. is fully entangled if it is neither biseparable nor fully separable.

GME is the strongest form of entanglement, that is, all qubits in the system are indeed entangled with each other. The size of the genuinely entangled quantum system becomes a figure of merit for assessing the advancement of quantum devices in the competition among various realizations.

Definition 4 (genuine multipartite entanglement)**.** A state possesses *genuine multipartite entanglement* (GME) if it is outside of S_2. A state possesses $\mathcal{P}$-genuine entanglement if it is outside of $S_b^{\mathcal{P}}$. A state ρ possesses $\mathcal{P}$-genuine entanglement iff $\rho \notin S_b^{\mathcal{P}}$.

Since $S_b^{\mathcal{P}_2} \subset S_b$, GME is a stronger claim than full entanglement. For a state with full entanglement, it is possible to prepare it by mixing bi-separable states with different bipartitions Compared with genuine entanglement, multipartite entanglement structure still lacks a systematic exploration, due to the rich and complex structures of n-partite system. Unfortunately, it remains an open problem of efficient entanglement-structure detection of general multipartite quantum states.

Rather than qualitatively determining (bi)separability, there are measures to quantify entanglement.

Definition 5 (concurrence)**.**

By going through all possible partitions, one can investigate higher level entanglement structures, such as entanglement intactness (non-separability), which quantifies how many pieces in the n-partite state are separated. To benchmark our technological progress towards the generation of largescale genuine multipartite entanglement, it is thus essential to determine the corresponding entanglement depth.

Definition 6 (Entanglement intactness, depth)**.** the entanglement intactness of a state ρ to be m, if and only if $\rho \notin S_{m+1}$ and $\rho \in S_m$. When the entanglement intactness is 1, the state possesses genuine multipartite entanglement; and when the intactness is n, the state is fully separable. k-producible.

graph state is an important large class of multipartite states in quantum information, because (connected) graph states represent a large class of genuine multipartite entangled states that have concise representations. Typical graph states include cluster states, GHZ states, and the states involved in error correction (toric code). It worth noting that 2D cluster (rectangular lattice graph) state is the universal resource for the measurement based quantum computation (MBQC) [8]. The entanglement in a graph state is related to the topology of its underlying graph [9].

Remark 1. LU, LC equivalence, local operations and classical communication (LOCC), local unitary/rotation

B. Entanglement detection

PPT criterion [7] Classically, the hardness of determining the bipartite separability. Another widely used one is the k-symmetric extension hierarchy [15, 16], which is presently one of the most powerful criteria, but hard to compute in practice due to its exponentially growing complexity with k.[??] In order to apply the PPT criterion (the minimum eigenvalue of the partial-transposed density matrix), the full density matrix must be available. However, quantum state tomography requires an exponential number of measurements.

However, up to now, no general solution for the separability problem is known. Similar to the PPT condition, the p_3-PPT condition applies to mixed states and is completely independent of the state in question. This is a key distinction from entanglement witnesses, which can be more powerful, but which **usually require detailed prior information about the state**. From this data set, the PT-moments p_n can be estimated without having to reconstruct the density matrix ρ_{AB}, and with a significantly smaller number of experimental runs M than required for full quantum state tomography. c.f. **??, ??**

Theorem 2 ([10])**.** *The weak membership problem for the convex set of separable normalized bipartite density matrices is* NP-*Hard.* **Input:** *unknown state?? formal definition of the problem [11]*

However, we do not know approximately correct complexity? quantum complexity? machine learning (data)? for entanglement () problem? multipartite?

Problem 1 (Entanglement detection)**.** Entanglement detection

- **Input**: a **unknown** state $|\psi\rangle$ (or with prior knowledge, with kinds of noise: noise noise, bit/phase-flip, local unitary $\hat{U}_A\hat{U}_B\hat{U}_C|\psi\rangle$, LOCC?); an (actual) state ρ' from experiment that is close to a **known/target** (general multipartite) state $|\psi\rangle$,

- **Output**: separable or entangled ??? $S_f^{\mathcal{P}}$? $S_b^{\mathcal{P}}$ the certified lower-order entanglement among several subsystems could be still useful for some quantum information tasks. entanglement structure genuine multipartite entanglement?? (intactness, depth)

difficulty: multi(n)-partite, high-dimensional (qudit) [12], pure/mixed state, with/out prior knowledge, universal?, non-stabilizer [6], certain partition

Bell inequalities as the oldest tool to detect entanglement. Originally, Bell inequalities were designed to rule out local hidden variable (LHV) models.

Definition 7 (CHSH inequality)**.** CHSH inequality (game) ...;

$$\hat{\mathbf{p}} = (\mathbb{1}, a_0 b_0, a_0 b_0', a_0' b_0, a_0' b_0'), \quad a_0 = \hat{Z}, a_0' = \hat{X}, b_0 = (\hat{X} - \hat{Z})/\sqrt{2}, b_0 = (\hat{X} + \hat{Z})/\sqrt{2}, \tag{2}$$

features as the input. CHSH operator $W_{\text{CHSH}} := \hat{\mathbf{p}} \cdot \mathbf{w}_{\text{CHSH}}$ with $\mathbf{w}_{\text{CHSH}} = \{\pm 2, 1, -1, 1, 1\}$

However, even for two-qubit systems there exist entangled states which do not violate any Bell inequality. [13] For example, the maximally-entangled Bell state can maximally violate the CHSH inequality, but this state mixed with certain extent white noise $(2/3)$ don't violate the CHSH inequality despite it is still entangled.

does not require any a priori knowledge about the quantum state. For $\text{Tr}(\rho_A^m)$, an important application of multivariate trace estimation [5] is to entanglement spectroscopy [14] [15] [16] - deducing the full set of eigenvalues of ρ_A. The smallest eigenvalue of diagnoses whether ψ_{AB} is separable or entangled [17]. The well-known identity (related to the replica trick originating in spin glass theory)

$$\text{Tr}\Big(\hat{U}^\pi(\rho_1 \otimes \cdots \otimes \rho_m)\Big) = \text{Tr}(\rho_1 \cdots \rho_m) \tag{3}$$

where the RHS is the multivariate trace and $\hat{U}^\pi$ is a unitary representation of the cyclic shift permutation. Direct entanglement detections, can be employed as sub-routines in quantum computation and realized by quantum circuits because it is naturally quantum data.

estimate the spectrum by quantum constant depth circuits, but this method only works for bipartite. (can we estimate concurrence by quantum circuit? quantum kernel SVM?) solve the quantum problem by quantum, without full tomography. unknown how to generalize to multipartite.

1. Entanglement witness based on fidelity (projection, local, nonlinear, stabilizer)

While various methods for constructing an entanglement witness exist, one of the most common is based on the fidelity of a state to a pure entangled state. Another approach for detecting multipartite entanglement is using entanglement witnesses. Different Bell inequalities can be regarded as entanglement witness for different types of entanglement in a multi-party entangled state. These witnesses can be quite useful to detect entanglement in the vicinity of graph states.

see Fig. 1 for relations. entanglement detection [18].

Definition 8 (entanglement witness)**.** Given an (unknown? known target state) quantum state (density matrix) ρ, the *entanglement witness* W is an obseverable such that

$$\mathbb{E}_\rho[W] \equiv \langle W \rangle \equiv \text{Tr}(W\rho) \geq 0, \forall \text{ separable} ; \quad \text{Tr}(W\rho) < 0, \text{ for some entangled} \tag{4}$$

[19], see Fig. 1

In a typical experiment one aims to prepare a pure state, $|\psi\rangle$, and would like to detect it as true multipartite entangled. While the preparation is never perfect, it is still expected that the prepared mixed state is in the proximity of $|\psi\rangle$. The usual way to construct entanglement witnesses using the knowledge of this state is

$$W_\psi = \alpha \mathbb{1} - |\psi\rangle\langle\psi| \tag{5}$$

where α is the smallest constant such that for every product state $\text{Tr}(\rho W) \geq 0$. projector-based witness [20]. However, it is generally difficult to evaluate the quantity $\text{Tr}(\rho_{\text{pre}} |\psi_{\text{tar}}\rangle\langle\psi_{\text{tar}}|)$ by the direct projection, as it is an entangled state. In order to measure the witness in an experiment, it must be decomposed into a sum of locally measurable operators. The number of local measurements in these decompositions seems to increase exponentially with the number of qubits.[??] local measurements [21] stabilizer [6] graph state [2]

Proposition 1 (Section 6.3 of [22])**.** *A state ρ is separable iff $\forall W, \mathrm{Tr}[\rho W] \geq 0$. Corollary, a state ρ is entangled iff $\exists W, \mathrm{Tr}[\rho W] < 0$. There is no entanglement witness that detects all entangled states.*

It is natural to ask how nonlinear entanglement witness [23] and the kernel method (nonlinear boundary) in machine learning can be applied.
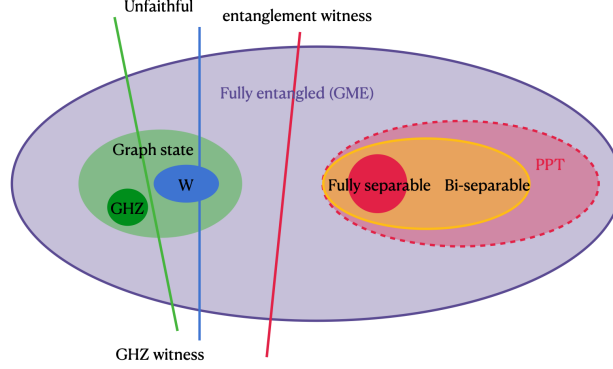

FIG. 1: (a) entanglement witness, PPT criterion [7], SVM (kernel)?. convex hull... The witness is depicted by the line in state space $\mathrm{Tr}(\rho W) = 0$

2. *Beyond fidelity and stabilizer witness (robustness)*

the authors coined the term faithful.

[12] For example, a witness specifically designed for a four-qubit compact cluster state [16] confirms, when its expectation value is negative, the presence of that particular state having a very specific density function, while a positive measured expectation value of that operator only provides information that the tested state is not a compact cluster state. Indeed, the same witness, if applied to a four-qubit linear cluster or GHZ [17] states, would result in a positive measured expectation value, even though these two states are both highly entangled [17, 18]. Hence, a witness is a threshold test that can only detect the presence of a specific state. In contrast to an entanglement monotone (e.g. the entanglement entropy [6]), which determines the amount of entanglement, a witness cannot be used to quantify entanglement.

Weilenmann et. al [24] proposed the idea of unfaithful states which systematically analyze entangled state with noise cannot be detected by fidelity witness. faithful states are useful for quantum teleportation. This shows that fidelity-based entanglement witnesses detect entanglement that is useful. [25] the faithfulness of a twoqubit state, allowing for a physical interpretation of unfaithful two-qubit states as exactly those entangled states that are not useful for teleportation. [26] [27]

Definition 9 (unfaithful state)**.**

They found that for $d \geq 3$ that almost all states in the Hilbert space are unfaithful. For $d > 5$, the authors find that all states they generated are entangled but at the same time unfaithful, regardless of what metric is used to sample them. Although there are nonlinear witnesses which also can detect entanglement in unfaithful states, they usually require more measurements []. Moreover, they can only be applied to bipartite systems, which means they cannot be generalized to detect genuine entanglement in multipartite states. Detecting Entanglement in Unfaithful States [28].

For non-stabilizer case, [29] [30] C is hard to compute? non-stabilizer state? SWAP? p_{noise} indicates the robustness of the algorithm (witness). the largest noise tolerance p_{limit} just related to the **chromatic number** of the graph (k local measurements) [2].(graph property) other noise (depolarization)? e.g., flip error, phase error?, local, random unitary transformation? find optimal (robustness) entanglement witness by classical machine learning (quantum circuit?) tradeoff between (white noise) tolerance (robustness) and efficiency (number of measurements).

III. CLASSICAL-QUANTUM HYBRID, END-TO-END DETECTION PROTOCOL

In this paper, we focus on the entanglement structure dectection for graph states. with training data

Problem 2 (Learning entanglement witness with training data)**.** Entanglement detection

- **Input**: specific entanglement structures y and corresponding synthetic data (density matrices ρ) with labels y

- **Output**: find the classifier with high accuracy and minimal features $\mathbf{x} :=$

The idea is to feed the classifier by a large amount of sampled trial states as well as their corresponding class labels.

A. Estimate classical features of quantum states

To make use of classical machine learning method, we need the classical **features** of quantum states. We cannot directly process quantum data (raw data). In our pipeline, we focus on classical shadow.

classical shadow [3]: estimate entanglment witness (fixed but unknown target state, e.g., tripartite GHZ) **Classical shadows (Clifford measurements) of logarithmic size allow for checking a large number of potential entanglement witnesses simultaneously**. Directly measuring M different entanglement witnesses requires a number of quantum measurements that scales (at least) linearly in M. In contrast, classical shadows get by with $\log(M)$-many measurements only. classical shadows are based on random Clifford measurements and do not depend on the structure of the concrete witness in question. In contrast, direct estimation crucially depends on the concrete witness in question and may be considerably more difficult to implement.

The brute force approach is to fully characterize a system by performing quantum state tomography and calculating separability measures from the recovered density matrix. Intuitively, a general tomography [31] that extract (recover) all information of a state requires exponential copies (samples/measurements).

Problem 3 (quantum state tomography)**.** Informally, quantum state tomography refers to the task of estimating complete description (density matrix) of an unknown N-dimensional quantum mixed state ρ within some error, given the ability to prepare and measure m copies $\rho^{\otimes m}$.

However, tomography is experimentally and computationally demanding; for a state consisting of n particles, with each residing in a d-dimensional Hilbert space, we would have to perform $M = \mathcal{O}(d^{2n})$ measurements.

Theorem 3 (lower bound of quantum state tomography?[32])**.** *Known fundamental lower bounds [66, 73] state that classical shadows of exponential size (at least) $T = \Omega(2^n/\epsilon^2)$ are required to ϵ-approximate ρ in trace distance.*

In quantum mechanics, interesting properties are often linear functions of the underlying density matrix ρ. For example, the fidelity with a pure target state, entanglement witnesses fit this framework.

Problem 4 (trace estimation)**.** related problems defined as follows

- **Input**: Given an observable (Hermitian) O and (copies of) a mixed state ρ or several states $(\rho', \ldots, \rho_m)$,

- **Output**: with error ϵ measured by trace distance (fidelity...), to estimate linear functions (mostly): the expectation value $\langle O \rangle = \text{Tr}(O\rho)$, entanglement witness, tomography; nonlinear functions: entropy; multivariate functions: $\text{Tr}(\rho_1 \cdots \rho_m)$, quantum kernel $\text{Tr}(\rho\rho')$, quadratic $\text{Tr}(O\rho_i \otimes \rho_j)$, fidelity $F(\rho, \rho')$, distance??;

Nevertheless, we usually only need specific properties of a target state rather than full classical descriptions about the state. This enables the possibility to shadow tomography.

Problem 5 (shadow tomography)**.** *shadow tomography*

- **Input**: an **unknown** N-dimensional mixed state ρ, M known 2-outcome measurements $E_1, \ldots, E_M$

- **Output**: estimate $\mathbb{P}[E_i \text{ accept } \rho]$ to within additive error ϵ, $\forall i \in [M]$, with $\geq 2/3$ success probability.

Theorem 4 (bounds of shadow tomography [33])**.** *It is possible to do shadow tomography using $\tilde{\mathcal{O}}(\frac{\log^4 M \cdot \log N}{\epsilon^4})$ copies. [no construction algorithm?] sample complexity lower bound $\Omega(\log(M) \cdot \epsilon^{-2})$,*

Remark 2 (compare shadow tomography with classical shadow [3])**.** While very efficient in terms of samples, Aaronson's procedure is very demanding in terms of quantum hardware - a concrete implementation of the proposed protocol requires **exponentially long quantum circuits** that act collectively on all the copies of the unknown state stored in a quantum memory.

1. Classical shadow and derandomized version

Inspired by Aaronson's shadow tomography [33], Huang et. al [3] introduce classical shadow. A classical shadow is a succinct classical description of a quantum state, which can be extracted by performing reasonably simple single-copy measurements on a reasonably small number of copies of the state. The classical shadow attempts to approximate this expectation value by an empirical average over T independent samples, much like Monte Carlo sampling approximates an integral.

Definition 10 (classical shadow). classical shadow (snapshots) ρ_{cs}

$$\rho_{cs} = \mathcal{M}^{-1}\left(U^{\dagger}\left|\hat{b}\right\rangle\left\langle\hat{b}\right|U\right) \tag{6}$$

such that we can predict the linear function with classical shadows

$$o_i = \text{Tr}(O_i\rho_{cs}) \text{ obeys } \mathbb{E}[o] = \text{Tr}(O_i\rho) \tag{7}$$

The classical shadow size required to accurately approximate all reduced r-body density matrices scales exponentially in subsystem size r, but is independent of the total number of qubits n.

Algorithm III.1: Classical Shadow (tomography): features for entanglement witness

---

input : an (unknown) density matrix ρ (many copies, black-box access to a circuit preparing a state), an entanglement witness (observable) W

output: classical shadow ρ_{cs}, $\text{Tr}(P_x\rho), \forall x \in \{I, X, Y, Z\}^n$

1 for $i = 1, 2, \ldots, N$ **do**

2 $\quad$ $\rho \mapsto \hat{U}\rho\hat{U}^{\dagger}$ $\qquad\qquad\qquad\qquad\qquad$ // apply a random unitary to rotate the state

3 $\quad$ $\mapsto |b\rangle\ldots$ $\qquad\qquad\qquad\qquad\qquad\qquad$ // perform a computational-basis measurement

4 $\quad$ $\rho_{cs} = \mathcal{M}^{-1}\left(\hat{U}^{\dagger}|b\rangle\langle b|\hat{U}\right)$ $\qquad\qquad$ // measurement outcome $|b\rangle \in \{0,1\}^n$, $\mathcal{M}$ quantum channel

5 return $S(\rho, N) = \left\{\rho_{cs_1} = \mathcal{M}^{-1}\left(\hat{U}_1^{\dagger}|b_1\rangle\langle b_1|\hat{U}_1\right), \ldots, \rho_{cs_N}\right\}$ $\qquad$ // call this array the classical shadow of ρ

/* estimate features $\qquad\qquad\qquad\qquad\qquad\qquad\qquad\qquad\qquad\qquad\qquad\qquad\qquad\qquad\qquad$ */

6 return estimation of $\text{Tr}(W\rho)$

A classical shadow is created by repeatedly performing a simple procedure: Apply a unitary transformation $\rho \mapsto \hat{U}\rho\hat{U}^{\dagger}$, and then measure all the qubits in the computational basis. The number of times this procedure is repeated is called the size of the classical shadow. The transformation U is randomly selected from an ensemble of unitaries, and different ensembles lead to different versions of the procedure that have characteristic strengths and weaknesses. Classical shadows with size of order $\log(M)$ suffice to predict M target functions $\{O_1, \ldots, O_M\}$.

Theorem 5 (Pauli/Clifford measurements). *Any procedure based on a fixed set of single-copy local measurements that can predict, with additive error ϵ, M arbitrary k-local linear function $\text{Tr}(O_i\rho)$, requires at least (lower bound) $\Omega(\log(M)3^k/\epsilon^2)$ copies of the state ρ. $\Omega(\log(M)\max_i \text{Tr}(O_i^2)/\epsilon^2)$*

Derandomization can and should be viewed as a refinement of the original classical shadows idea. [34] [16]

2. Estimate expectation by (classical/quantum) machine learning

[35] $\sigma_T(\rho(x_l))$ is the classical shadow representation of $\rho(x_l)$, a $2^n \times 2^n$ matrix that reproduces $\rho(x_l)$ in expectation over random Pauli measurements.

$$\{x_l \to \sigma_T(\rho(x_l))\}_{l=1}^N \tag{8}$$

Definition 11 (shadow kernel). given two density matrices (quantum states) ρ and ρ', *shadow kernel* [3] is

$$k_{\text{shadow}}(S_T(\rho), S_T'(\rho')) := \exp\left(\frac{\tau}{T^2}\sum_{t,t'=1}^{T}\exp\left(\frac{\gamma}{n}\sum_{i=1}^{n}\text{Tr}\left(\sigma_i^{(t)}\sigma_i^{(t')}\right)\right)\right) \tag{9}$$

where $S_T(\rho)$ is the classical shadow representation of ρ. The computation time for the inner product is $\mathcal{O}(nT^2)$, linear in the system size n and quadratic in T, the number of copies of each quantum state which are measured to construct the classical shadow.

Proposition 2 ([4]). *exist quantum advantage in machine learning (not significant, practical) ... discrete log, factoring...*

though, that while there is no large advantage in query complexity, a substantial quantum advantage in computational complexity is possible.

The quantum ML algorithm accesses the quantum channel $\mathcal{E}_\rho$ multiple times to obtain multiple copies of the underlying quantum state ρ. Each access to $\mathcal{E}_\rho$ allows us to obtain one copy of ρ. Then, the quantum ML algorithm performs a sequence of measurements on the copies of ρ to accurately predict $\text{Tr}(P_x\rho), \forall x \in \{I, X, Y, Z\}^n$.

Theorem 6 ([36]). *For M Pauli opertors, there is a (quantum) procedure estimate every expectation value $\text{Tr}(P_x\rho), \forall i = 1, \ldots, M$ within error ϵ under probability at least $1 - \delta$ by performing POVM measurements on $\mathcal{O}(\log(M/\delta)\epsilon^{-4})$ copies of the unknown quantum state ρ. ($M = 4^n$ implies linear copy for full tomography???) We rigorously show that, for any quantum process $\mathcal{E}$, observables O, and distribution $\mathcal{D}$, and for any quantum ML model, one can always design a classical ML model achieving a similar average prediction error such that N_C (number of experiments?) is larger than N_Q by at worst a small polynomial factor.*

*In contrast, for achieving accurate prediction on all inputs, we prove that **exponential quantum advantage is possible**. For example, to predict expectations of all **Pauli observables** (entanglement witness??) in an n-qubit system ρ, classical ML models require $2^{\Omega(n)}$ copies of ρ, but we present a quantum ML model using only $\mathcal{O}(n)$ copies.*

[3] [36] [4] [33]

	circuits	number of copies (measurements)
shadow tomography	exp circuit?	Theorem 4
classical shadow		
derandomized		better performance
quantum/classical ML		Q. advantage Theorem 6

TABLE I: complexity (measures) of different trace estimation methods

generative neural network [37]

B. Training a witness for certain entanglement with SVM

separability classifier by classical neural network [38]: input: sythetic random density matrices; output: a classical classifier for bipartite separable (independent of state??). (feature: synthetic density matrix with noise flatten as a real vector $\mathbf{x} \in \mathbb{R}^{d_A^2 d_B^2 - 1}$) (label: separable or entangled by PPT criterion [7], CHA), and then train the classifier to predict the class labels of new states that it has not encountered before. Previous methods **only detect a limited part of the state space**, e.g. different entangled states often require different entanglement witness. In contrast, this classifier can handle a variety?? of input states once properly trained Fig. 1. Bell inequaity and NN [13]. a linear Bell-like predictor by generalizing the CHSH operator $W_{\text{ml}} := \mathbf{P} \cdot \mathbf{w}_{\text{ml}}$ in Eq. (2) where the coefficients (or weights) $\mathbf{w}$ are determined by machine learning. tomographic ansatz better performance. training a universal classifier for multi-qubit, high-dimensional system is hard (boundary). it is difficult to generate general GME states or label general states. Tomography is necessary for universal entanglement detection with single-copy observables (non-adaptive schemes) [39]

classical SVM: This method the ability to obtain witnesses that require only local measurements even when the target state is a **non-stabilizer state** W state (normally need nonlocal measurements). feature: $\mathbf{x}_{\vec{k}}$ expectation of Pauli strings. the training of an SVM is convex; if a solution exists for the given target state and ansatz, the optimal SVM will be found. this SVM formalism allows for the programmatic removal of features, i.e., reducing the number of experimental measurements, in exchange for a lower tolerance to white noise, in a manner similar to [??]. SVM, (universal), 4 qubit [40]

classical machine learning (SVM, NN) with classical shadow [35]??: classify phase, predict ground state, entanglement? The quantum extension of this problem (classficiation/pattern recognition) is to replace the data points $\mathbf{x}_i$ with density matrices of quantum states ρ_i. Specifically, a quantum state classifier outputs a "label" associated with the state, for example, entangled or "unentangled". In actual experiments, we don't know entries of a density matrix. Instead, we need measurements or classical shadow as features of machine learning algorithms.

an ansatz for entanglement witness [30] (graph state entanglement)

$$W_{\text{ansatz}} := \sum_{\mathbf{p} \in \{I,X,Y,Z\}^n} w_{\mathbf{p}} \bigotimes_i^n \mathbf{p}_i \tag{10}$$

	# observables	weights	input state
entanglement witness	constant? few local	fixed	known
Bell (CHSH) inequality	constant	fixed	unknown
tomographic witness	4^n	trained	unknown
ML	??	trained	partially known

TABLE II: ansatz

c.f. quantum state tomography (Stokes parameters) **??**. An SVM allows for the construction of a hyperplane $\langle W \rangle = \sum_k w_k \mathbf{x}_k$ that clearly delineates between separable states and the target entangled state (bipartite and **tripartite qubit and qudit**); this hyperplane is a **weighted sum of observables ('features') whose coefficients are optimized during the training of the SVM**.

We focus on kernel methods, as they not only provide provable guarantees, but are also very flexible in the functions they can learn. For example, recent advancements in theoretical machine learning show that training neural networks with large hidden layers is equivalent to training an ML model with a particular kernel, known as the neural tangent kernel [41].

Algorithm III.2: ansatz + classical shadow (..) + Classical learning (SVM)

---

input : an entanglement witness (observable) ansatz $W_{D_{\mathrm{ML}}} = \mathbf{w} \cdot \vec{\sigma}$; classical shadow? (features) with label (training data)

output: classifier $\mathbf{w}$; entanglement structure? decision separble; classify phase

```
// ----------------------------------------- training phase ------------------------------------------
```
1 for $i = 1, 2, \ldots, m$ **do**
2   kernel estimation   `// classical kernel`
3   SVM   `// SVM`
4   **return** parameters $\mathbf{w}$ (SVM hyperplane)   `// parameters of the separating hyperplane in the feature space`

         `// call classical shadow to extract features from quantum states`
5 return $\mathbf{w} \cdot \vec{\sigma} < 0$: separable `/* predict`   `*/`
```
// ========================================= testing phase ========================================= //
```

Theorem 7. *On quantum computers, evaluating the trace distances is probably hard since even judging whether ρ and ρ' have large or small trace distance is known to be QSZK-complete [42], where QSZK (quantum statistical zero-knowledge) is a complexity class that includes BQP (bounded-error quantum polynomial time). [43]*

IV. NUMERICAL SIMULATION

A. Data preparation and state generation

multi-partite entangled state: generate synthetic (engineered) data from (random graph?). separable state from randomly ... QuTiP library [44]; quantum circuit [45]

entangled states generation: Bell, GHZ, W state, graph (cluster) state

$$\cos(\theta)\left|00\right\rangle + \sin(\theta)e^{\mathrm{i}\phi}\left|11\right\rangle, \ \cos(\theta)\left|01\right\rangle + \sin(\theta)e^{\mathrm{i}\phi}\left|10\right\rangle \tag{11}$$

separable states generation

- 2-qubit: bipartite

- Training data for $\rho_b^{(1,2,3)}$ generated by sampling over the Hilbert-Schmidt-distributed space of single-qubit and bi-qubit density matrices. As for the entangled state, we again use the Werner state to generate the training data for that class of states.

$$\rho_{A|B|C}, \ \rho_{A|BC}, \ \rho_{AB|C}, \ \rho_{B|AC} \quad \left|rand\right\rangle_A \otimes \left|rand\right\rangle_B, \ \left|rand\right\rangle_A \otimes \left|entangle\right\rangle_{BC}, \tag{12}$$
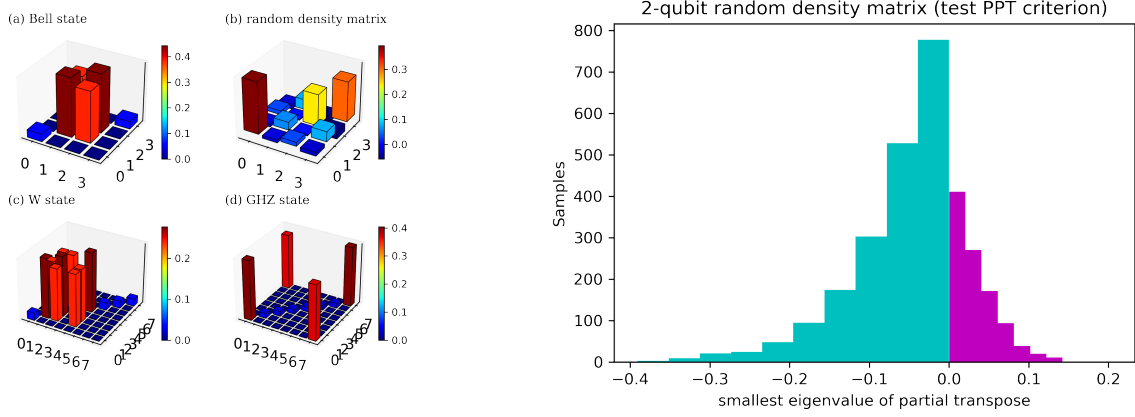
FIG. 2: data praparation: random states (a) three-qubit W state, (b) GHZ state with white noise (c) (d) (e) PPT

B. Classification accuracy and comparison

1. Hyperparameters and settings

We consider a set of different regularization parameters,...

The goal of RFE is to eliminate non-essential features by recursively considering smaller and smaller subsets of the original features using a greedy algorithm. Initially, RFE takes the SVM we trained and ranks the coefficients by their magnitudes, with the lowest one pruned away; then the model is trained again with the remaining features.
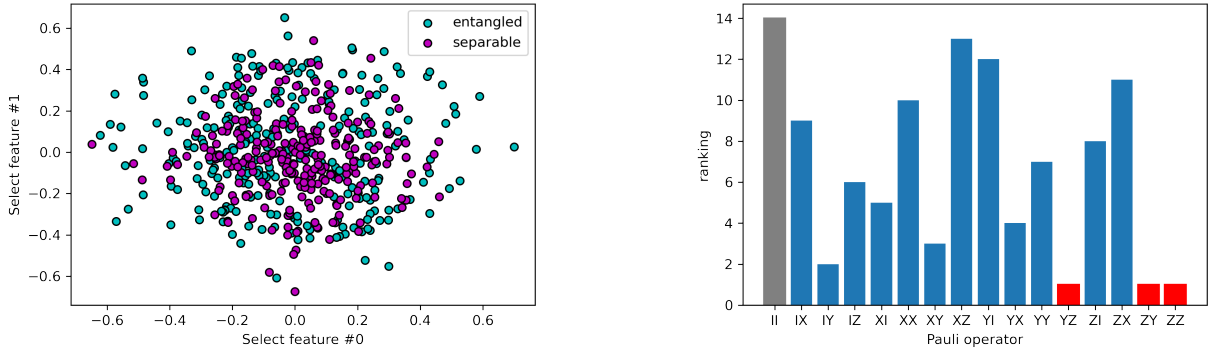

FIG. 3: (a) two-dimensional embedding: feature space, recursive feature elimination; (b) feature ranking

2. Results, feature elimination

performance of different methods: for any state ρ_s with only bipartite entanglement, $\mathrm{Tr}(O\rho_s) \leq 0.5$, while for any state ρ_s with at most W-type entanglement, $\mathrm{Tr}(O\rho_s) \leq 0.75$. Therefore verifying that $\mathrm{Tr}(O\rho) \geq 0.5$ certifies that ρ has tripartite entanglement, while $\mathrm{Tr}(O\rho) > 0.75$ certifies that ρ has GHZ-type entanglement. [46]

V. EXPERIMENTS

future: experimental (photonic) implementation with a few qubits (generation, verification) [47]. fully entangled graph state (ring of 16 qubits) IBM by measuring negativity [48] optical lattice [49] (homogeneous, restricted measurement, different noise channels; detect GME, full entanglement). classical shadow experiments [50] [16]
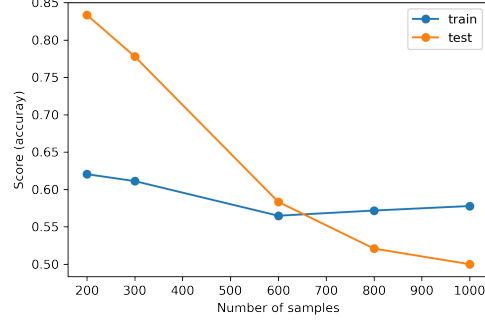
FIG. 4: accuracies (variance) VS different data sizes

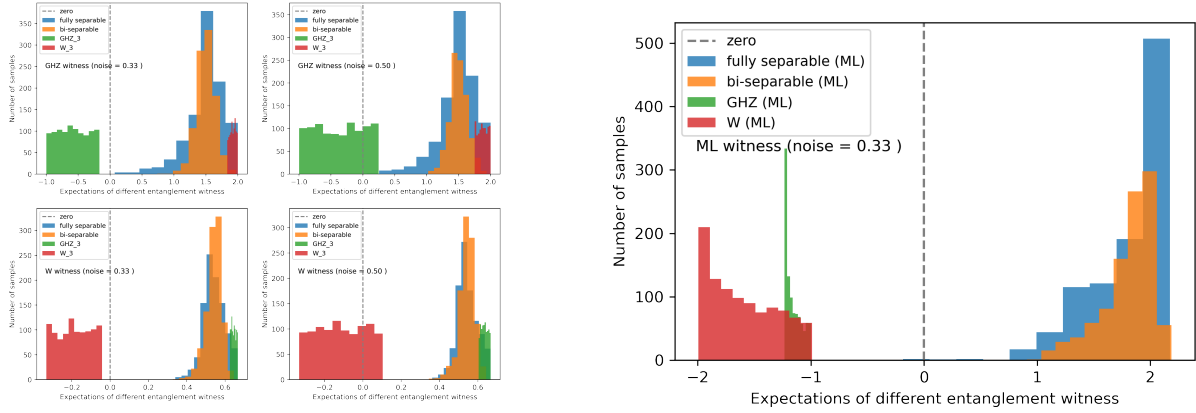FIG. 5: number of features VS number of qubits (n). feature elimination

FIG. 6: (a) compare different methods: Bell inequality, witness, ML ansatz; different white noise limit, unfaithful state; (b) ML witness for unfaithful (large white noise), non-stabilizer (W) state

VI. CONCLUSION AND DISCUSSION

[1] R. Horodecki, P. Horodecki, M. Horodecki, and K. Horodecki, Rev. Mod. Phys. **81**, 865 (2009), arXiv:quant-ph/0702225.
[2] Y. Zhou, Q. Zhao, X. Yuan, and X. Ma, npj Quantum Inf **5**, 83 (2019).
[3] H.-Y. Huang, R. Kueng, and J. Preskill, Nat. Phys. **16**, 1050 (2020), arXiv:2002.08953 [quant-ph].
[4] H.-Y. Huang, M. Broughton, M. Mohseni, R. Babbush, S. Boixo, H. Neven, and J. R. McClean, Nat Commun **12**, 2631 (2021), arXiv:2011.01938 [quant-ph].
[5] Y. Quek, M. M. Wilde, and E. Kaur, Multivariate trace estimation in constant quantum depth (2022), arXiv:2206.15405 [hep-th, physics:quant-ph].
[6] G. Tóth and O. Gühne, Phys. Rev. A **72**, 022340 (2005).
[7] M. Horodecki, P. Horodecki, and R. Horodecki, Physics Letters A **223**, 1 (1996), arXiv:quant-ph/9605038.
[8] H. J. Briegel, D. E. Browne, W. Dür, R. Raussendorf, and M. V. den Nest, Nature Phys **5**, 19 (2009), arXiv:0910.1116.
[9] M. Hein, W. Dür, J. Eisert, R. Raussendorf, M. V. den Nest, and H.-J. Briegel, Entanglement in Graph States and its Applications (2006), arXiv:quant-ph/0602096.

[10] L. Gurvits, Classical deterministic complexity of Edmonds' problem and Quantum Entanglement (2003), arXiv:quant-ph/0303055.

[11] L. M. Ioannou, Quantum Inf. Comput. **7**, 335 (2007), arXiv:quant-ph/0603199.

[12] S. Sciara, C. Reimer, M. Kues, P. Roztocki, A. Cino, D. J. Moss, L. Caspani, W. J. Munro, and R. Morandotti, Phys. Rev. Lett. **122**, 120501 (2019).

[13] Y.-C. Ma and M.-H. Yung, npj Quantum Inf **4**, 34 (2018), arXiv:1705.00813 [quant-ph].

[14] A. K. Ekert, C. M. Alves, D. K. L. Oi, M. Horodecki, P. Horodecki, and L. C. Kwek, Phys. Rev. Lett. **88**, 217901 (2002), arXiv:quant-ph/0203016.

[15] S. Johri, D. S. Steiger, and M. Troyer, Phys. Rev. B **96**, 195136 (2017), arXiv:1707.07658.

[16] A. Elben, R. Kueng, H.-Y. Huang, R. van Bijnen, C. Kokail, M. Dalmonte, P. Calabrese, B. Kraus, J. Preskill, P. Zoller, and B. Vermersch, Phys. Rev. Lett. **125**, 200501 (2020), arXiv:2007.06305 [cond-mat, physics:quant-ph].

[17] P. Horodecki and A. Ekert, Phys. Rev. Lett. **89**, 127902 (2002), arXiv:quant-ph/0111064.

[18] O. Gühne and G. Toth, Physics Reports **474**, 1 (2009), arXiv:0811.2803 [cond-mat, physics:physics, physics:quant-ph].

[19] B. M. Terhal, Physics Letters A **271**, 319 (2000), arXiv:quant-ph/9911057.

[20] M. Bourennane, M. Eibl, C. Kurtsiefer, S. Gaertner, H. Weinfurter, O. Guehne, P. Hyllus, D. Bruss, M. Lewenstein, and A. Sanpera, Phys. Rev. Lett. **92**, 087902 (2004), arXiv:quant-ph/0309043.

[21] G. Toth and O. Guehne, Phys. Rev. Lett. **94**, 060501 (2005), arXiv:quant-ph/0405165.

[22] T. Heinosaari and M. Ziman, *The Mathematical Language of Quantum Theory: From Uncertainty to Entanglement*, 1st ed. (Cambridge University Press, 2011).

[23] O. Gühne and N. Lütkenhaus, Phys. Rev. Lett. **96**, 170502 (2006).

[24] M. Weilenmann, B. Dive, D. Trillo, E. A. Aguilar, and M. Navascués, Phys. Rev. Lett. **124**, 200502 (2020), arXiv:1912.10056 [quant-ph].

[25] O. Gühne, Y. Mao, and X.-D. Yu, Phys. Rev. Lett. **126**, 140503 (2021), arXiv:2008.05961 [quant-ph].

[26] G. Riccardi, D. E. Jones, X.-D. Yu, O. Gühne, and B. T. Kirby, Exploring the relationship between the faithfulness and entanglement of two qubits (2021), arXiv:2102.10121 [quant-ph].

[27] X.-M. Hu, W.-B. Xing, Y. Guo, M. Weilenmann, E. A. Aguilar, X. Gao, B.-H. Liu, Y.-F. Huang, C.-F. Li, G.-C. Guo, Z. Wang, and M. Navascués, Phys. Rev. Lett. **127**, 220501 (2021).

[28] Y. Zhan and H.-K. Lo, Detecting Entanglement in Unfaithful States (2021), arXiv:2010.06054 [quant-ph].

[29] Y. Zhang, Y. Tang, Y. Zhou, and X. Ma, Phys. Rev. A **103**, 052426 (2021), arXiv:2012.07606 [quant-ph].

[30] E. Y. Zhu, L. T. H. Wu, O. Levi, and L. Qian, Machine Learning-Derived Entanglement Witnesses (2021), arXiv:2107.02301 [quant-ph].

[31] J. Altepeter, E. Jeffrey, and P. Kwiat, in *Advances In Atomic, Molecular, and Optical Physics*, Vol. 52 (Elsevier, 2005) pp. 105–159.

[32] J. Haah, A. W. Harrow, Z. Ji, X. Wu, and N. Yu, IEEE Trans. Inform. Theory , 1 (2017).

[33] S. Aaronson, in *Proc. 50th Annu. ACM SIGACT Symp. Theory Comput.*, STOC 2018 (Association for Computing Machinery, New York, NY, USA, 2018) pp. 325–338, arXiv:1711.01053.

[34] H.-Y. Huang, R. Kueng, and J. Preskill, Phys. Rev. Lett. **127**, 030503 (2021), arXiv:2103.07510 [quant-ph].

[35] H.-Y. Huang, R. Kueng, G. Torlai, V. V. Albert, and J. Preskill, Provably efficient machine learning for quantum many-body problems (2021), arXiv:2106.12627 [quant-ph].

[36] H.-Y. Huang, R. Kueng, and J. Preskill, Phys. Rev. Lett. **126**, 190505 (2021), arXiv:2101.02464 [quant-ph].

[37] Y. Zhu, Y.-D. Wu, G. Bai, D.-S. Wang, Y. Wang, and G. Chiribella, Flexible learning of quantum states with generative query neural networks (2022), arXiv:2202.06804 [quant-ph].

[38] S. Lu, S. Huang, K. Li, J. Li, J. Chen, D. Lu, Z. Ji, Y. Shen, D. Zhou, and B. Zeng, Phys. Rev. A **98**, 012315 (2018), arXiv:1705.01523 [quant-ph].

[39] D. Lu, T. Xin, N. Yu, Z. Ji, J. Chen, G. Long, J. Baugh, X. Peng, B. Zeng, and R. Laflamme, Phys. Rev. Lett. **116**, 230501 (2016), arXiv:1511.00581 [quant-ph].

[40] S. V. Vintskevich, N. Bao, A. Nomerotski, P. Stankus, and D. A. Grigoriev, Classification of four-qubit entangled states via Machine Learning (2022), arXiv:2205.11512 [quant-ph].

[41] A. Jacot, F. Gabriel, and C. Hongler, Neural Tangent Kernel: Convergence and Generalization in Neural Networks (2020), arXiv:1806.07572 [cs, math, stat].

[42] J. Watrous, Quantum Computational Complexity (2008), arXiv:0804.3401 [quant-ph].

[43] R. Chen, Z. Song, X. Zhao, and X. Wang, Quantum Sci. Technol. **7**, 015019 (2022), arXiv:2012.05768 [math-ph, physics:quant-ph].

[44] J. R. Johansson, P. D. Nation, and F. Nori, Computer Physics Communications **184**, 1234 (2013), arXiv:1110.0573.

[45] B. Li, S. Ahmed, S. Saraogi, N. Lambert, F. Nori, A. Pitchford, and N. Shammah, Quantum **6**, 630 (2022), arXiv:2105.09902 [quant-ph].

[46] A. Acin, D. Bruss, M. Lewenstein, and A. Sanpera, Phys. Rev. Lett. **87**, 040401 (2001), arXiv:quant-ph/0103025.

[47] H. Lu, Q. Zhao, Z.-D. Li, X.-F. Yin, X. Yuan, J.-C. Hung, L.-K. Chen, L. Li, N.-L. Liu, C.-Z. Peng, Y.-C. Liang, X. Ma, Y.-A. Chen, and J.-W. Pan, Phys. Rev. X **8**, 021072 (2018).

[48] Y. Wang, Y. Li, Z.-q. Yin, and B. Zeng, npj Quantum Inf **4**, 46 (2018), arXiv:1801.03782.

[49] Y. Zhou, B. Xiao, M.-D. Li, Q. Zhao, Z.-S. Yuan, X. Ma, and J.-W. Pan, npj Quantum Inf **8**, 1 (2022).

[50] T. Zhang, J. Sun, X.-X. Fang, X.-M. Zhang, X. Yuan, and H. Lu, Experimental quantum state measurement with classical shadows (2021), arXiv:2106.10190 [physics, physics:quant-ph].

[51] C. Bădescu, R. O'Donnell, and J. Wright, Quantum state certification (2017), arXiv:1708.06002 [quant-ph].

[52] A. Montanaro and R. de Wolf, A Survey of Quantum Property Testing (2018), arXiv:1310.2035 [quant-ph].
[53] S. Ben-David, A. M. Childs, A. Gilyén, W. Kretschmer, S. Podder, and D. Wang, 2020 IEEE 61st Annu. Symp. Found. Comput. Sci. FOCS , 649 (2020), arXiv:2006.12760.
[54] N. M. Kriege, F. D. Johansson, and C. Morris, Appl Netw Sci 5, 6 (2020), arXiv:1903.11835 [cs, stat].
[55] L. Bai, L. Rossi, A. Torsello, and E. R. Hancock, Pattern Recognition 48, 344 (2015).
[56] V. Havlicek, A. D. Córcoles, K. Temme, A. W. Harrow, A. Kandala, J. M. Chow, and J. M. Gambetta, Nature 567, 209 (2019), arXiv:1804.11326.
[57] M. Schuld and N. Killoran, Phys. Rev. Lett. 122, 040504 (2019), arXiv:1803.07128 [quant-ph].
[58] Y. Liu, S. Arunachalam, and K. Temme, Nat. Phys. 17, 1013 (2021), arXiv:2010.02174 [quant-ph].
[59] J. R. Glick, T. P. Gujarati, A. D. Corcoles, Y. Kim, A. Kandala, J. M. Gambetta, and K. Temme, Covariant quantum kernels for data with group structure (2021), arXiv:2105.03406 [quant-ph].
[60] X. Gao and L.-M. Duan, Nat Commun 8, 662 (2017), arXiv:1701.05039 [cond-mat, physics:quant-ph].

Appendix A: Definitions

Definition 12 (density matrix)**.** pure state $|\psi\rangle$; A quantum state ρ is defined to be a positive operator $\rho \in \text{End}(V)$ with $\text{Tr}(\rho) = 1$. density matrix ρ (trace one, Hermitian, PSD)...

Definition 13 (POVM)**.** A positive-operator valued measurement (POVM) M consists of a set of positive operators that sum to the identity operator $\mathbb{1}$. When a measurement $M = \{E_1, \ldots, E_k\}$ is applied to a quantum state ρ, the outcome is $i \in [k]$ with probability $p_i = \text{tr}(\rho E_i)$. observables ... $\mathbb{E}[x] \equiv \langle O_x \rangle := \text{tr}(O_x \rho)$

Definition 14 (positive, semidefinite)**.** denoted $X \preceq Y$ provided $Y - X$ is positive

Definition 15 (partial trace)**.** reduced density matrix $\rho_A = \text{Tr}_B(\rho_{AB})$

Remark 3. a pure (bipartite) state is entangled iff the reduced state $\rho^A = \text{Tr}_A(\rho)$ is mixed. The mixedness of this reduced state allows one to quantify the amount of entanglement in this state.

Definition 16 (partial transpose)**.** [7] The partial transpose (PT) operation - acting on subsystem A - is defined as

$$|k_A, k_B\rangle\langle l_A, l_B|^{\mathsf{T}_A} := |l_A, k_B\rangle\langle k_A, l_B| \tag{A1}$$

where $\{|k_A, k_B\rangle\}$ is a product basis of the joint system AB.

Definition 17 (maximally entangled)**.** a state vector is *maximually entangled* iff the reduced state at one qubit is maximally mixed, i.e., $\text{Tr}_A(|\psi\rangle\langle\psi|) = \frac{1}{2}$.

Definition 18 (Schmidt measure)**.** Consider the following bipartite pure state, written in Schmidt form:

$$|\psi\rangle = \sum_i^r \sqrt{\lambda_i} \left|\phi_i^A\right\rangle \otimes \left|\phi_i^B\right\rangle \tag{A2}$$

where $\{|\phi_i^A\rangle\}$ is a basis for $\mathcal{H}_A$ and $\{|\phi_i^A\rangle\}$ for $\mathcal{H}_B$. The strictly positive values $\sqrt{\lambda_i}$ in the Schmidt decomposition are its *Schmidt coefficients*. The number of Schmidt coefficients, counted with multiplicity, is called its *Schmidt rank*, or Schmidt number. (Schmidt rank ?? $\text{SR}^A(\psi) = \text{rank}(\rho_\psi^A)$) Schmidt measure is minimum of $\log_2 r$ where r is number of terms in an expansion of the state in product basis.

Definition 19 (entropy)**.** In quantum mechanics (information), the von Neumann *entropy* of a density matrix is $H_N(\rho) := -\text{Tr}(\rho \log \rho) = -\sum_i \lambda_i \log(\lambda_i)$; In classical information (statistical) theory, the Shannon entropy of a probability distribution P is $H_S(P) := -\sum_i P(x_i) \log P(x_i)$. relative entropy (divergence)

Definition 20 (entanglement entropy)**.** The bipartite *von Neumann entanglement entropy* S is defined as the von Neumann entropy of either of its reduced density matrix ρ_A. For a pure state $\rho_{AB} = |\Psi\rangle\langle\Psi|_{AB}$, it is given by

$$E(\Psi_{AB}) = S(\rho_A) = -\text{Tr}(\rho_A \log \rho_A) = -\text{Tr}(\rho_B \log \rho_B) = S(\rho_B) \tag{A3}$$

where $\rho_A = \text{Tr}_B(\rho_{AB})$ and $\rho_B = \text{Tr}_A(\rho_{AB})$ are the reduced density matrices for each partition. With Schmidt decomposition (Eq. (A2)), the entropy of entanglement is simply $-\sum_i p_i^2 \log(p_i)$. the nth Renyi entropy, $S_n = \frac{1}{n-1} \log(R_n)$ where $R_n = \text{Tr}(\rho_A^n)$

Example 1. The Schmidt measure for any multi-partite GHZ states is 1, because there are just two terms. Schmidt measure for 1D, 2D, 3D-**??** is $\lfloor \frac{N}{2} \rfloor$. Schmidt measure of tree is the size of its minimal vertex cover[??].

Definition 21 (fidelity). Given a pair of states (target ρ and prepared ρ'), Uhlmann fidelity $F(\rho, \rho') := \text{Tr}\left(\sqrt{\sqrt{\rho}\rho'\sqrt{\rho}}\right) \equiv \left\|\sqrt{\rho}\sqrt{\rho'}\right\|_1$, where $\sqrt{\rho}$ dentoes the positive semidefinite square root of the operator ρ. (infidelity $1 - F(\rho, \rho')$) For any mixed state ρ and pure state $|\psi\rangle$, $F(\rho, |\psi\rangle\langle\psi|) = \sqrt{\langle\psi|\rho|\psi\rangle} \equiv \sqrt{\text{Tr}(\rho\,|\psi\rangle\langle\psi|)}$ which can be obtained by the Swap-test[?]. linear fidelity or overlap $F(\rho, \rho') := \text{tr}(\rho\rho')$.

different distance measures [51]

Notation 4 (norm). Schatten p-norm $\|x\|_p := (\sum_i |x_i|^p)^{1/p}$. Euclidean norm l_2 norm; Spectral (operator) norm $\|\mathbf{x}\|_\infty$; Trace norm $\|A\|_{\text{Tr}} \equiv \|A\|_1 := \text{Tr}(|A|) \equiv \text{Tr}\left(\sqrt{A^\dagger A}\right)$, $|A| := \sqrt{A^\dagger A}$, $p = 1$; Frobenius norm $\|A\|_F := \sqrt{\text{Tr}(A^\dagger A)}$, $p = 2$; Hilbert-Schmidt norm $\|A\|_{HS} := \sqrt{\sum_{i,j} A_{ij}^2} =? \sum_{i \in I} \|Ae_i\|_H^2$; Hilbert-Schmidt inner product $\langle A, B \rangle_{\text{HS}} := \text{Tr}(A^\dagger B)$, Frobenius inner product $\langle A, B \rangle_{\text{F}} := \text{Tr}(A^\dagger B)$? (in finite-dimensionala Euclidean space, the HS norm is identical to the Frobenius norm) Although the Hilbert-Schmidt distance is arguably not too meaningful, operationally, one can use Cauchy-Schwarz to relate it to the very natural trace distance. shadow norm ...

Definition 22 (distance). For mixed states, trace distance $d_{\text{tr}}(\rho, \rho') := \frac{1}{2}\|\rho - \rho'\|_1$. For pure states, $d_{\text{tr}}(|\psi\rangle, |\psi'\rangle) := \frac{1}{2}\||\psi\rangle\langle\psi| - |\psi'\rangle\langle\psi'|\|_1 = \sqrt{1 - |\langle\psi|\psi'\rangle|^2}$. fidelity and trace distance are related by the inequalities

$$1 - F \leq D_{\text{tr}}(\rho, \rho') \leq \sqrt{1 - F^2} \tag{A4}$$

variation distance of two distribution $d_{var}(p, p') := \frac{1}{2}\sum_i |p_i - p_i'| = \frac{1}{2}\|p - p'\|_1$. l_2 distance ... Hellinger distance ... HS distance $D_{\text{HS}}(\rho, \rho') := \|\rho - \rho'\|_{\text{HS}} = \sqrt{\text{Tr}((\rho - \rho')^2)}$

denote a group by $\mathbb{G}$ and a subgroup $\mathbb{H}$.

Definition 23 (Pauli group).

Definition 24 (Clifford group).

Definition 25 (Stabilizer). An observable S_k is a stabilizing operator of an n-qubit state $|\psi\rangle$ if the state $|\psi\rangle$ is an eigenstate of S_k with eigenvalue 1,

A stabilizer set $S = \{S_1, \ldots, S_n\}$ consisting of n mutually commuting and independent stabilizer operators is called the set of stabilizer "generators".

Many highly entangled n-qubit states can be uniquely defined by n stabilizing operators which are locally measurable, i.e., they are products of Pauli matrices. A stabilizer S_i is an n-fold tensor product of n operators chosen from the one qubit Pauli operators $\{\mathbb{1}, X, Y, Z\}$. An n-partite(qubit) graph state can also be uniquely determined by n independent stabilizers, $S_i := X_i \bigotimes_{j \in n} Z_j$, which commute with each other and $\forall i, S_i |G\rangle = |G\rangle$.?? The graph state is the unique eigenstate wtih eignevalue of $+1$ for all the n stabilizers. As a result, a graph state can be written as a product of stailizer projectors, $|G\rangle\langle G| = \prod_{i=1}^n \frac{S_i + \mathbb{1}}{2}$. Stabilizer formalism

Example 2 (GHZ). For GHZ state: $|\text{GHZ}\rangle := \frac{1}{\sqrt{2}}(|0\rangle^{\otimes n} + |1\rangle^{\otimes n})$, the projector based witness

$$W_{\text{GHZ}_3} = \frac{1}{2}\mathbb{1} - |\text{GHZ}\rangle\langle\text{GHZ}| \tag{A5}$$

requires four measurement settings. For three-qubit GHZ state [21], the local measurement witness

$$W_{\text{GHZ}_3} := \frac{3}{2}\mathbb{1} - \hat{X}^{(1)}\hat{X}^{(2)}\hat{X}^{(3)} - \frac{1}{2}\left(\hat{Z}^{(1)}\hat{Z}^{(2)} + \hat{Z}^{(2)}\hat{Z}^{(3)} + \hat{Z}^{(1)}\hat{Z}^{(3)}\right) \tag{A6}$$

This witness requires the measurement of the $\left\{\hat{\sigma}_x^{(1)}, \hat{\sigma}_x^{(2)}, \hat{\sigma}_x^{(3)}\right\}$ and $\left\{\hat{\sigma}_z^{(1)}, \hat{\sigma}_z^{(2)}, \hat{\sigma}_z^{(3)}\right\}$ settings. For n-qubit case, detect genuine n-qubit entanglement close to GHZ_n

$$W_{\text{GHZ}_n} = (n-1)\mathbb{1} - \sum_{k=1}^n S_k(\text{GHZ}_n) \tag{A7}$$

where $\hat{S}_k$ is the Stabilizer ... [6] Detecting Genuine Multipartite Entanglement with Two Local Measurements [21]

Definition 26 (graph state). Given a simple graph (undirected, unweighted, no loop and multiple edge) $G = (V, E)$, a graph state is constructed as from the initial state $|+\rangle^{\otimes n}$ corresponding to n vertices. Then, apply controlled-Z gate to every edge, that is $|G\rangle := \prod_{(i,j) \in E} \text{cZ}_{(i,j)} |+\rangle^{\otimes n}$ with $|+\rangle := (|0\rangle + |1\rangle)/\sqrt{2}$.

Question 1. *how to relate graph state entanglement to graph property test ..??. (graph kernel??) [9]. witness; bounds; graph property? vertex cover? Hamiltonian cycle of a graph state?*

	$\lvert\text{GHZ}_3\rangle$	$\lvert W_3\rangle$	$\lvert CL_3\rangle$	$\lvert\psi_2\rangle$	$\lvert\mathcal{D}_{2,4}\rangle$	$\lvert\text{GHZ}_n\rangle$	$\lvert W_3\rangle$	$\lvert G_n\rangle$
α	1/2	2/3	1/2	3/4	2/3	1/2	$(n-1)/n$	1/2
maximal p_{noise}	4/7	8/21	8/15	4/15	16/45	$1/2 \cdot (1-1/2^n)^{-1}$		
local measurements	4	5	9	15	21	$n+1$	$2n-1$	depend on graphs

<div align="center">TABLE III: [18]</div>

Appendix B: Machine learning background

Notations: The (classical) training data (for supervised learning) is a set of m data points $\left\{(\mathbf{x}^{(i)}, y^{(i)})\right\}_{i=1}^{m}$ where each data point is a pair $(\mathbf{x}, y)$. Normally, the input (e.g., an image) $\mathbf{x} := (x_1, x_2, \ldots, x_d) \in \mathbb{R}^d$ is a vector where d is the number of *features* and its *label* $y \in \Sigma$ is a scalar with some discrete set Σ of alphabet/categories. For simplicity and the purpose of this paper, we assume $\Sigma = \{-1, 1\}$ (binary classification).

1. Support vector machine

SVM is a typical supervised learning algorithm for classification. Taking the example of classifying cat/dog images, supervised learning means we are given a dataset in which every image is labeled either a cat or a dog such that we can find a function classifying new images with high accuracy. More precisely, the training dataset is a set of pairs of features X and their labels y. In the image classification case, features are obtained by transforming all pixels of an image into a vector. In SVM, we want to find a linear function, that is a hyperplane which separates cat data from dog data. So, the prediction label is given by the sign of the inner product (projection) of the hyperplane and the feature vector. We can observe that the problem setting of image classification by SVM is quite analogous to entanglement detection, where input data are quantum states now and the labels are either entangled or separable.

Definition 27 (SVM)**.** Given a set of (binary) labeled data, support vector machine (SVM) is designed to find a hyperplane (a linear function) such that maximize the margin between two partitions...

$$\max_{\mathbf{w}} \|\mathbf{w}\|^2 \text{ s.t. } \forall i, y^{(i)} \cdot (\mathbf{w} \cdot \mathbf{x} + b) \geq 1. \tag{B1}$$

Lagrange multipliers α

$$L = \frac{1}{2}\|\mathbf{w}\|^2 - \sum_{i}^{m} \alpha^{(i)}\left(\mathbf{w} \cdot \mathbf{x}^{(i)} + b\right) + \sum_{i}^{m} \alpha^{(i)} \tag{B2}$$

a. kernel method

However, note that SVM is only a linear classifier. while most real-world data, such as cat/dog images and entangled/separable quantum states are not linearly separable. For example, with this two dimension dataset, we are unable to find a hyperplane to separate red points from the purple points very well. Fortunately, there is a very useful tool called kernel method or kernel trick to remedy this drawback. The main idea is mapping the features to a higher dimensional space such that they can be linearly separated in the high dimensional feature space. Just like this example, two dimensional data are mapped to the three dimensional space. Now, we can easily find the separating plane. With SVM and kernel methods, we expect to find a generic and flexible way for entanglement detection. kernel

Definition 28 (kernel)**.** In general, the kernel function $k : \mathcal{X} \times \mathcal{X} \to \mathbb{R}$ measures the similarity between two input data points by an inner product

$$k(\mathbf{x}, \mathbf{x}') := \langle \phi(\mathbf{x}), \phi(\mathbf{x}') \rangle \tag{B3}$$

If the input $\mathbf{x} \in \mathbb{R}^d$ (conventional machine learning task, e.g., image classification), the feature map $\phi(\mathbf{x}) : \mathbb{R}^d \to \mathbb{R}^n$ ($d < n$) from a low dimensional space to a higher dimensional space. The corresponding kernel (Gram) matrix $\mathbf{K}$ should be a positive, semidefinite (PSD) matrix, i.e. all eigenvalues are non-negative

Example 3 (kernels)**.** Some common kernels: the polynomial kernel $k_{\text{poly}}(\mathbf{x}, \mathbf{x}') := (1 + \mathbf{x} \cdot \mathbf{x}')^q$ with feature map $\phi(\mathbf{x})$ ... The Gaussian kernel $k_{\text{gaus}}(\mathbf{x}, \mathbf{x}') := \exp\left(-\gamma\|\mathbf{x} - \mathbf{x}'\|_2^2\right)$ with an infinite dimensional feature map $\phi(\mathbf{x})$. An important feature of kernel method is that kernels can be computed efficiently without evaluating feature map (might be infinite dimension) explicitly.

similarity measures? advantages? why? (isomorphism?)

Definition 29 (divergence)**.** KL divergence (relative entropy): measure the distance (similarity) between two probability distributions:

$$D_{\mathrm{KL}}(P||Q) := \sum P(x) \log(P(x)/Q(x)) \tag{B4}$$

symmetric version: Jensen-Shannon divergence (machine learning)

$$D_{\mathrm{JS}}(P||P') := \frac{1}{2}(D_{\mathrm{KL}}(P||M) + D_{\mathrm{KL}}(P'||M)) \equiv H_S(M) - \frac{1}{2}(H_S(P) - H_S(P')) \tag{B5}$$

where $M = (P + P')/2$ and Shannon entropy H_S. Analogously, quantum Jensen-Shannon divergence D_{QJS} of two density matrices can be defined...

$$D_{\mathrm{QJS}}(\rho||\rho') := H_V(\rho_M) - \frac{1}{2}(H_V(\rho) - H_V(\rho')) \tag{B6}$$

as a quantum graph kernel (ρ induced by quantum random walk)

Definition 30 (geometric difference)**.**

$$g(K^1||k^2) = \sqrt{\left\| \sqrt{K^2}(K^1)^{-1}\sqrt{K^2} \right\|_\infty} \tag{B7}$$

where $\|\cdot\|_\infty$ is the spectral norm.

b. Graph kernel

Definition 31 (graph property)**.** monotone ...

Example 4 (colorable)**.** k-colorable is a graph property, i.e., allow for a coloring of the vertices with k colors such that no two adjacent vertices have the same color. A graph is bipartite iff 2-colorable. other graph properties: isomorphism; vertex cover; Hamiltonian cycle ...

Problem 6 (graph property test)**.** **promise**: the input graph either has a property, or is ϵ-far from having the property, meaning that we must change at least an ϵ fraction of the edges to make the property hold.

Theorem 8 (bounds for graph property test)**.**

Question 2. *[52] Is there any graph property which admits an exponential quantum speed-up? [53] depends on input model (query adjacency matrix/list)*

Graphs is another kind of data which is fundamentally different from a real value vector because of vertex-edge relation and graph isomorphism. So, graph kernel [54] need additional attention.

Definition 32 (graph kernel)**.** given a pair of graphs (G, G'), *graph kernel* is $k(G, G') =$. quantum graph kernel $k(G, G') = |\langle G|G'\rangle|^2$?? [55]

c. Quantum kernel

related works:

- quantum kernel method: estimate kernels by quantum algorithms (circuits) [56] [57]: for classical problem (data)

- rigorous and robust quantum advantage of quantum kernel method in SVM [58]. group structured data [59]

- power of data in quantum machine learning [4]: input??? projected quantum kernel

Definition 33 (quantum kernel)**.** quantum kernel with quantum feature map $\phi(\mathbf{x}) : \mathcal{X} \to |\phi(\mathbf{x})\rangle\langle\phi(\mathbf{x})|$

$$k_Q(\rho, \rho') := |\langle\phi(\mathbf{x})|\phi(\mathbf{x}')\rangle|^2 = \left| \langle 0|\hat{U}_{\phi(\mathbf{x})}^\dagger \hat{U}_{\phi(\mathbf{x}')}|0\rangle \right|^2 =? \operatorname{Tr}(\rho\rho') \equiv \langle\rho, \rho'\rangle_{\mathrm{HS}} \tag{B8}$$

where $\hat{U}_{\phi(\mathbf{x})}$ is a quantum circuit or physics process that encoding an input $\mathbf{x}$. In quantum physics, quantum kernel is also known as transition amplitude (quantum propagator);

Proposition 3 ([4])**.** *If a classical algorithm without training data can compute (label) $y = f(x) = \langle x|\hat{U}_{\mathrm{QNN}}^\dagger O U_{\mathrm{QNN}}|x\rangle$ (with amplitude encoding) efficiently (poly time in ...) for any $\hat{U}_{\mathrm{QNN}}$ and O, then* BPP = BQP *(which is believed unlikely).*

Proposition 4 ([4])**.** *Training an arbitrarily deep quantum neural network $\hat{U}_{\mathrm{QNN}}$ with a trainable observable O is equivalent to training a quantum kernel method with kernel $k_Q(\mathbf{x}, \mathbf{x}') = \operatorname{Tr}(\rho(\mathbf{x})\rho'(\mathbf{x}'))$*

Definition 34 (projected quantum kernel)**.** ....

2. Neural network

a. neural network and kernel

Definition 35 (neural tagent kernel)**.** neural tangent kernel [41]: proved to be equivalent to deep neural network [60] in the limit ...

$$k_{\mathrm{NT}}\left(S_T(\rho_l), \tilde{S}_T(\rho_{l'})\right) = \left\langle \phi^{(\mathrm{NT})}(S_T(\rho_l)), \phi^{(\mathrm{NT})}(\tilde{S}_T(\rho_l)) \right\rangle \tag{B9}$$

b. quantum neural network

Appendix C: Hardness assumptions

Definition 36 (NP)**.** NP, NP-hard, NP-complete

Definition 37 (#P)**.** #P

Definition 38 (QMA)**.** QMA

Definition 39 (BPP)**.** BPP

Definition 40 (BQP)**.** BQP